

Band Structure of Graphite and de Haas-van Alphen Effect

J. W. McCLURE

National Carbon Research Laboratories, National Carbon Company,* Cleveland, Ohio

(Received July 3, 1957)

The de Haas-van Alphen effect in the magnetic susceptibility of graphite has been interpreted by applying the susceptibility formula for general bands of Lifschitz and Kosevich to the band model of Slonczewski. The majority electrons and holes are responsible for the two periods of oscillation of the susceptibility. The analysis yields information concerning the band structure: (1) the total band overlap is about 0.03 eV, (2) the energy difference between the two doubly degenerate bands at the corner of the Brillouin zone is about 0.025 eV, (3) γ_0 must be larger than about 1.2 eV, and (4) the relation $\gamma_1 = 0.04\gamma_0^2$ holds approximately (where both γ 's are in eV and correspond to Wallace's notation). Calculated carrier densities are 2.4×10^{-5} per atom for electrons and 1.8×10^{-5} per atom for holes, in rough agreement with estimates made from galvanomagnetic data. Rough agreement with electron specific-heat data is also obtained.

1. INTRODUCTION

THE current carriers in graphite occupy a very small fraction of the Brillouin zone. Because of this, and because of the large anisotropy of the crystal lattice, it is possible to write formulas for the energy as a function of wave number which involve six unknown constants. The band model is described in Sec. 2. Some of the band parameters are determined in Sec. 3 by using information gained from de Haas-van Alphen experiments. The results are consistent with the galvanomagnetic data and the low-temperature specific heat.

The crystal structure of graphite is depicted in Fig. 1. The atoms are arranged in hexagonal layer planes, the spacing between nearest neighbors in the planes being 1.42 Å. The planes are stacked in *abab* order, 3.37 Å apart. The a_0 and c_0 distances are 2.46 Å and 6.74 Å, respectively. Note that, of the four atoms in a unit cell, *A* and *A'* have neighbors directly above and below in adjacent planes and that *B* and *B'* do not. (For convenience, we always imagine a Cartesian axis system embedded in the crystal, with the *z* axis vertical and parallel to the c_0 axis of the crystal.) The Brillouin zone is a thin hexagonal pillbox, shown in Fig. 2. Because of

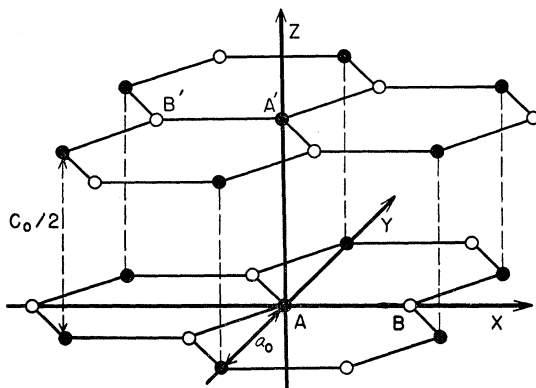


FIG. 1. The graphite crystal lattice.

* A Division of Union Carbide Corporation.

the large anisotropy in the crystal structure, it is a useful starting approximation to discuss the properties of a single layer. This was first done by Wallace,¹ who found that the highest occupied band and the lowest unoccupied band (which we shall call the valence and conduction bands, respectively) are degenerate in energy at the six zone corners (the Brillouin zone for a single layer being simply a two-dimensional hexagon). Later calculations of the single-layer band structure by Coulson and Taylor,² Lomer,³ and Corbato⁴ agree that the valence and conduction bands are degenerate at the zone corners. Furthermore, there are no other bands with energies near the degeneracy energy, so that the only part of the band structure important for transport phenomena is the region near the zone corners.

Interaction between layers lifts some of the degeneracy. The splitting is small (about 0.1 eV) compared to the band width (about 15 eV), but is appreciable compared to the kinetic energies of the carriers. In the three-dimensional case there are two conduction and two valence bands (not counting spin degeneracy), two of which are required by symmetry to be degenerate along the vertical zone edges (*HH* and *H'H'*). Wallace's

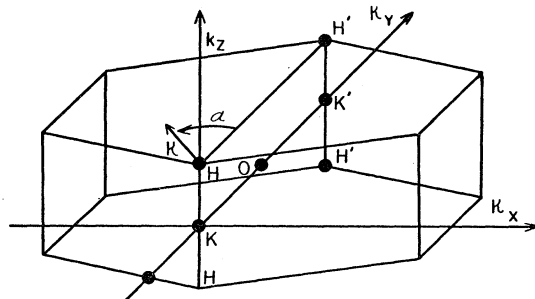


FIG. 2. The reduced Brillouin zone for graphite, showing the coordinate system used.

¹ P. R. Wallace, Phys. Rev. **71**, 622 (1947).

² C. A. Coulson and R. Taylor, Proc. Phys. Soc. (London) **A65**, 815 (1952).

³ W. M. Lomer, Proc. Roy. Soc. (London) **A227**, 330 (1955).

⁴ F. J. Corbato, Quarterly Progress Report, Solid State and Molecular Theory Group (Massachusetts Institute of Technology, No. 21, 1956) (unpublished), p. 23.

three-dimensional calculation,¹ which was a tight-binding calculation taking into account nearest-neighbor interactions only, has one conduction band degenerate with one valence band along the vertical zone edges, but no band overlap. A calculation by Johnston⁵ which took into account more distant neighbors gave extra degeneracies near the zone edges and a small overlap between valence and conduction bands. A later calculation by Johnston⁶ reveals a larger band overlap due to the dependence of the degeneracy energy on k_z (along HH and $H'H'$). The possibility of overlap of this kind has been pointed out by Slonczewski⁷ and also found by Horton and Tauber.⁸

In the face of the increasing complexity of the band structure, it is natural to turn to group theory to establish which types of structure are possible. Group-theoretical studies have been made for the single-layer Brillouin zone by Lomer³ and Slonczewski,⁷ and for the three-dimensional zone by Carter.⁹ Slonczewski⁷ and Slonczewski and Weiss¹⁰ (henceforth called SW) have combined group theory and perturbation theory in a calculation which will be described in the next section.

2. BAND STRUCTURE MODEL

The basic idea of the Slonczewski-Weiss model can be stated very simply: previous calculations show that the interesting part of the Brillouin zone is quite near the vertical zone edges (no further from the zone edge than about one percent of the distance from the zone edge to zone center); thus, it is sensible to make a Taylor expansion of the Hamiltonian in terms of κ_x and κ_y (distances from the zone edge in the x and y directions). However, in the z direction, a Fourier expansion of the Hamiltonian is made as the layer planes are widely separated and the series is rapidly convergent (a case of ideal tight-binding). From a study of the symmetry of the lattice, they find it possible to write the eigenfunctions corresponding to any point on a zone edge in terms of Bloch sums of single-layer eigenfunctions. For points not on the edge they use the method of Bouckaert, Smoluchowski, and Wigner¹¹ in which the change in the Hamiltonian is given to first order by $\hbar\mathbf{\kappa}\cdot\mathbf{p}/m$. In the above, $\mathbf{\kappa}$ is the shortest vector from the zone edge to the point in question, and \mathbf{p} is the momentum matrix for the states on the zone edge (at $\mathbf{k}-\mathbf{\kappa}$). The method can be extended to second order in $\mathbf{\kappa}$ by use of Van Vleck per-

turbation theory¹² as Shockley did for cubic lattices.¹³ The same " $\mathbf{k}\cdot\mathbf{p}$ " method has been recently used with considerable success in the study of the valence bands of several semiconductors.¹⁴ Thus, the form of the momentum matrix is the key to the type of band structure, and it has been a major concern in the work of Slonczewski and Weiss.

The labeling of the states on the zone edge which we adopt is based on that of SW and is explained below: Band 1 corresponds to the sum of Bloch waves made up from $2p_z$ orbitals based on A and A' atoms and is generally the highest in energy; Band 2 corresponds to the difference of the same Bloch waves based on A and A' atoms and is generally the lowest in energy. Bands 1 and 2 are degenerate on the zone corners (H and H'). Bands 31 and 32 correspond to Bloch waves made up of $2p_z$ orbitals based on B' and B atoms, respectively. Bands 31 and 32 are degenerate everywhere on the zone edge.

In writing the Hamiltonian we shall use a set of dimensionless variables, $\alpha = \tan^{-1}(-\kappa_x/\kappa_y)$, $\sigma = \frac{1}{2}\sqrt{3}a_0|\kappa|$, $\xi = k_z c_0$. In these variables, Wallace's S can be written near the zone corner as $S = \sigma \exp(i\alpha)$. To give an idea of relative magnitudes, the σ value for the zone center is 3.6, and height of the zone in the same units is $\sqrt{3}\pi a_0/c_0 = 1.99$. The number of carriers of both spins contained in two cylinders of radius $2\sigma/\sqrt{3}a_0$ and height $2\pi/c_0$ (there are two such complete cylinders in a zone) is $0.092\sigma^2$ per atom or $1.05 \times 10^{22}\sigma^2$ per cm^3 . In pure graphite, we shall see that maximum σ values for carriers are of the order of 0.03 and carrier concentrations are of the order of 10^{-5} per atom.

In the notation established, the Hamiltonian is

$$H = \begin{pmatrix} E_1 & 0 & H_{13} & H_{13}^* \\ 0 & E_2 & H_{23} & -H_{23}^* \\ H_{13}^* & H_{23}^* & E_3 & H_{33} \\ H_{13} & -H_{23} & H_{33}^* & E_3 \end{pmatrix}, \quad (2.1a)$$

where the order of rows and columns is 1, 2, 31, 32, and

$$E_1 = \gamma_1 \Gamma + \Delta, \quad (2.1b)$$

$$E_2 = -\gamma_1 \Gamma + \Delta, \quad (2.1c)$$

$$E_3 = \gamma_2(1 + \cos\xi) = \frac{1}{2}\gamma_2 \Gamma^2, \quad (2.1d)$$

$$H_{13} = 2^{-\frac{1}{2}}(-\gamma_0 + \gamma_4 \Gamma)\sigma \exp(i\alpha), \quad (2.1e)$$

$$H_{23} = 2^{-\frac{1}{2}}(\gamma_0 + \gamma_4 \Gamma)\sigma \exp(i\alpha), \quad (2.1f)$$

$$H_{33} = \gamma_3 \Gamma \sigma \exp(i\alpha). \quad (2.1g)$$

In the above, we have put $\Gamma = 2 \cos(\frac{1}{2}\xi)$. The Hamiltonian is taken from SW with the approximation that only the first nonvanishing k_z -dependent term is kept in each matrix element. As written, it applies to the zone edge HH ; the complex conjugate applies to $H'H'$. SW

⁵ D. F. Johnston, Proc. Roy. Soc. (London) **A227**, 349 (1955).

⁶ D. F. Johnston, Proc. Roy. Soc. (London) **A237**, 48 (1956).

⁷ J. C. Slonczewski, Ph.D. thesis, Rutgers University, 1955 (University Microfilms, Ann Arbor, Michigan, 1956, Mic 56-2314).

⁸ G. K. Horton and G. E. Tauber (unpublished).

⁹ J. L. Carter, Ph.D. thesis, Cornell University, 1953 (unpublished).

¹⁰ J. C. Slonczewski and P. R. Weiss, Phys. Rev. **99**, 636(A) (1955).

¹¹ Bouckaert, Smoluchowski, and Wigner, Phys. Rev. **50**, 58 (1936).

¹² J. H. Van Vleck, Phys. Rev. **33**, 467 (1929).

¹³ W. Shockley, Phys. Rev. **78**, 173 (1950).

¹⁴ See, for example, Dresselhaus, Kip, and Kittel, Phys. Rev. **98**, 368 (1955) or E. O. Kane, J. Phys. Chem. Solids **1**, 82 (1956).

worked out the Hamiltonian to first order in σ . The form of the second-order Hamiltonian is given by simply squaring the first-order Hamiltonian, and does not produce any qualitatively different structure. The magnitude of a typical second-order term can be inferred from Johnston's work to be about equal to the free-electron value of $0.5\sigma^2$ eV, which is about 5×10^{-4} eV for a σ value of 0.03. This is to be compared with $\gamma_0\sigma$ or $\gamma_0^2\sigma^2/\gamma_1$, each of which is about 0.1 eV at the same σ value. Spin-orbit coupling is ignored as SW estimate the splitting so produced as about 10^{-4} eV. The same band model has been used by Nozières in discussing cyclotron resonance in graphite.¹⁵

There are six constants in Eqs. (2.1) which we shall discuss individually. The quantity γ_0 which we have defined to be the same as Wallace's γ_0 , is the most important in determining the dependence of energy on σ . It is also the only parameter in the single-layer case. Wallace quotes an estimate for γ_0 by Coulson (based on chemical evidence) of 0.9 eV. Lomer and Johnston estimate 3 eV. SW calculated the momentum matrix element and arrived at 2.3 eV. Corbato's calculation yields a value of 3.2 eV. Finally, an estimate based on the magnitude of the magnetic susceptibility gives 2.6 eV.¹⁶

The parameter γ_1 represents the chief splitting of bands caused by the interlayer interaction. Wallace estimated 0.1 eV and Johnston's work yields 0.35 eV. The quantity Δ reflects the fact that the A and B atom sites are different. It was pointed out by Carter and Krumhansl¹⁷ that it is not required by symmetry that all four bands be degenerate at H and H' . They estimated that Δ is about 0.01 eV. The parameter γ_2 is responsible for most of the band overlap. Johnston obtains a value of -0.007 eV from the mixing of $2p_z$ orbitals with other types, due to the interlayer interaction. However, Horton and Tauber estimate 0.001 eV from next-nearest-plane overlap effects. As the two effects compete, the sign is in doubt. The quantity γ_3 gives rise to the anisotropy in the xy plane and the extra degeneracies near the zone edge found by Johnston. Johnston's work yields an estimate of 0.13 eV for γ_3 . The term is present in Wallace's Hamiltonian as γ_1' but was ignored in computing the energy. The parameter γ_4 does not have a qualitative effect on the band structure but could have an appreciable quantitative effect. It would be equal to γ_3 if the orbitals on A and B atoms were identical; as the differences are probably slight, it is very nearly equal to γ_3 . This term was also included as a γ_1' term in Wallace's Hamiltonian.

In discussing the energy spectrum of (2.1), we first ignore γ_3 and γ_4 . Then the energy is independent of α and is worked out by SW to be

$$E = \frac{1}{2}(E_1 + E_3) \pm \left[\frac{1}{4}(E_1 - E_3)^2 + \gamma_0^2\sigma^2 \right]^{\frac{1}{2}}, \quad (2.2a)$$

$$E = \frac{1}{2}(E_2 + E_3) \pm \left[\frac{1}{4}(E_2 - E_3)^2 + \gamma_0^2\sigma^2 \right]^{\frac{1}{2}}. \quad (2.2b)$$

The dependence of E on σ is called "hyperbolic" by SW, in contrast to the more familiar "parabolic" dependence. Note that the two formulas (2.2a) and (2.2b) differ only by the sign of $\cos(\frac{1}{2}\xi)$. Thus, for easy visualization we may plot one of the formulas in a double-height Brillouin zone. Figure 3 shows a three-dimensional plot of E versus σ and ξ for formula (2.2b). The case shown is for positive values of all the parameters; it is seen that for pure graphite, holes would be located along the central part of HH and electrons would be located near the points H .

Inclusion of γ_4 would produce only additional warping of the energy surface depicted in Fig. 3. However, introduction of γ_3 produces additional structure. The secular equation derived from (2.1) then no longer factors into two quadratic equations for all \mathbf{k} . At present it is un-instructive to examine the solution to the quartic equation, so we look instead at two special cases. For certain planes in k space (given by $\alpha = \frac{1}{3}n\pi$) the secular equation still factors and we obtain Johnston's solution.

$$E = \frac{1}{2}(E_2 + E_3 - \gamma_3\Gamma\sigma \cos 3\alpha) \pm \left[\frac{1}{4}(E_2 - E_3 + \gamma_3\Gamma\sigma \cos 3\alpha)^2 + (\gamma_0 + \gamma_4\Gamma)^2\sigma^2 \right]^{\frac{1}{2}}. \quad (2.3)$$

The above equation gives all four roots when we let ξ run over the double zone.

In the case that E_1 and E_2 are well separated from E_3 , we can solve (2.1) by perturbation theory and find the explicit angular dependence of the two bands derived from 31 and 32. We find

$$E = E_3 + A\sigma^2 \pm [B^2\sigma^4 + 2B\sigma^3\gamma_3\Gamma \cos 3\alpha + \sigma^2\gamma_3^2\Gamma^2]^{\frac{1}{2}}, \quad (2.4a)$$

where

$$A = \frac{1}{2} \left[\frac{(\gamma_0 - \gamma_4\Gamma)^2}{E_3 - E_1} + \frac{(\gamma_0 + \gamma_4\Gamma)^2}{E_3 - E_2} \right], \quad (2.4b)$$

$$B = \frac{1}{2} \left[\frac{(\gamma_0 + \gamma_4\Gamma)^2}{E_3 - E_2} - \frac{(\gamma_0 - \gamma_4\Gamma)^2}{E_3 - E_1} \right]. \quad (2.4c)$$

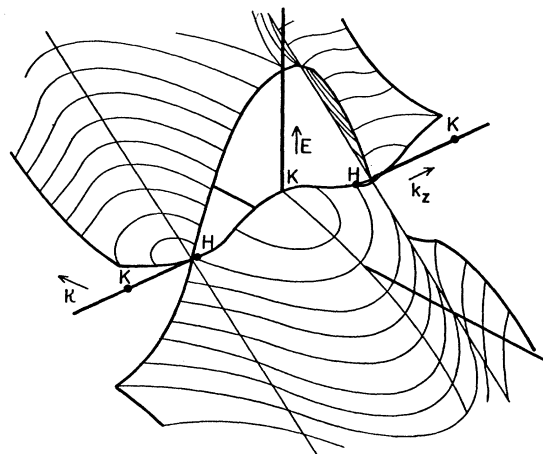


FIG. 3. The energy versus wave vector for the four-parameter model, using the double-zone convention. The energy is plotted vertically and the wave-vector coordinates are as shown in Fig. 2.

¹⁵ P. P. Nozières, Bull. Am. Phys. Soc. Ser. II, 1, 321 (1956).

¹⁶ J. W. McClure, Phys. Rev. 104, 666 (1956).

¹⁷ J. L. Carter and J. A. Krumhansl, J. Chem. Phys. 21, 2238 (1953).

In the foregoing, ξ is restricted to the first zone (if ξ is allowed in the second zone the same two bands are reproduced). It is seen that for $\alpha = \frac{1}{3}n\pi$, (2.4a) gives two overlapping parabolas, and for other α 's the extra crossing of bands disappears. Note that there are three satellite minima (or maxima) in addition to the central one. With the estimates of parameter values given previously, the scale of the energy variation due to γ_3 is about 0.001 eV, and the variation is important for σ values of about 0.001.

We are now in a position to construct a picture of the Fermi surface in pure graphite, which is shown in Fig. 4. In constructing the figure, we have used the Fermi surfaces given by Fig. 3 (with the electron surfaces translated back into the central zone) and applied the trigonal warping due to γ_3 . We conclude this section by noting that the group theory-perturbation theory treatment did not uncover any qualitative type of behavior not already reported. It does, of course, include all previous calculations as special cases. Its greatest value is that it provides fairly simple, general formulas and contains the minimum number of adjustable parameters.

3. DE HAAS-VAN ALPHEN EFFECT

The low-temperature oscillatory behavior of the magnetic susceptibility of graphite has been studied by Shoenberg¹⁸ and by Berlincourt and Steele,¹⁹ with substantial agreement. Shoenberg analyzed his data on the basis of constant tensor mass theory. Recently Lifshitz and Kosevich²⁰ have presented a theory which is valid for general band structures. The dependence of the susceptibility on temperature and magnetic field strength is the same in both theories, so that Shoenberg's analysis can be utilized by constructing a translation key for the parameters involved in the two theories. In the general theory, the oscillatory susceptibility is determined by the properties of the band structure in the region where the cross section of the Fermi surface perpendicular to the magnetic field has its maximum (or minimum) value. The period of oscillation in inverse magnetic field is given by

$$P = 2\pi e / A_m \hbar c \rightarrow \beta / \zeta, \quad (3.1)$$

where A_m is the maximum cross section (measured in rationalized wave numbers squared), β is the double effective Bohr magneton and ζ is the Fermi energy. The equality holds for the general case and the arrow indicates the value taken for the case of constant tensor mass. The dependence of amplitude on field strength and temperature is specified by the ratio of the magnetic energy-level spacing to the thermal energy. The energy

¹⁸ D. Shoenberg, Phil. Trans. Roy. Soc. (London) **245**, 1 (1952).
¹⁹ T. G. Berlincourt and M. C. Steele, Phys. Rev. **98**, 956 (1955).
²⁰ I. M. Lifshitz and A. M. Kosevich, J. Exptl. Theoret. Phys. (U.S.S.R.) **29**, 730 (1955) [translation: Soviet Phys. JETP **2**, 636 (1956)].

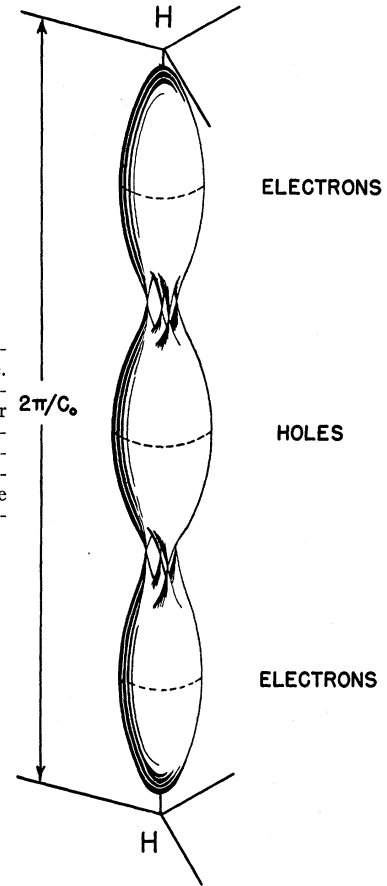


FIG. 4. The Fermi surface for pure graphite. The central surface contains holes and the outer surfaces contain electrons. The length-to-width ratio of each surface is about 13. The trigonal anisotropy is exaggerated for clarity.

level spacing is given by

$$\Delta E = (2\pi e \mathcal{H} / \hbar c) \partial E / \partial A \rightarrow e \hbar \mathcal{H} / m_{\perp} c, \quad (3.2)$$

where the derivative is evaluated at the maximum cross section of the Fermi surface, m_{\perp} is the effective mass perpendicular to the c_0 axis (we are treating here only the case with the magnetic field parallel to the c_0 axis), and \mathcal{H} is the magnetic field strength. The magnitude of the amplitude of oscillation depends upon a quantity

$$|\partial^2 A / \partial k_z^2| \rightarrow m_{\parallel} / m_{\perp} 2\pi, \quad (3.3)$$

where this derivative is also evaluated at the maximum cross section, and m_{\parallel} is the effective mass parallel to the c_0 axis. In principle, information can be gained from the phases of the oscillations, however, these quantities were not determined precisely in Shoenberg's experiment and will not be discussed here.

Shoenberg finds two distinct contributions to the de Haas-van Alphen effect, the two transverse masses being $0.036m_0$ and $0.07m_0$. We identify these two contributions as those of electrons and holes respectively on the basis of the cyclotron resonance data of Galt *et al.*,²¹ which has been analyzed by Lax and Zeiger²²

²¹ Galt, Yager, and Dail, Phys. Rev. **103**, 1586 (1956).
²² B. Lax and H. J. Zeiger, Phys. Rev. **105**, 1466 (1957).

TABLE I. Calculated band parameters for graphite. The values of the band parameters chosen to fit the de Haas-van Alphen data are given for assumed values of γ_0 . Note that the upper half of the table refers to positive γ_2 , and the lower half refers to negative γ_2 . The $\cos\frac{1}{2}\xi$ column refers to the position of the maximum cross section of the Fermi surface (for electrons in the upper half, and for holes in the lower). The calculated "de Haas-van Alphen" mass anisotropies and carrier densities for electrons (n_e) and holes (n_h) are also given.

γ_0 (ev)	γ_1 (ev)	γ_2 (ev)	Δ (ev)	ζ (ev)	$\cos\frac{1}{2}\xi_m$	$(m_{11}/m_{\perp})_e$	$(m_{11}/m_{\perp})_h$	n_e (atoms ⁻¹)	n_h (atoms ⁻¹)
1.17	0.041	0.033	0.075	0.055	0.62	105	80	2.1	1.4
1.50	0.085	0.019	0.035	0.028	0.50	125	120	2.3	1.7
2.00	0.162	0.017	0.018	0.024	0.48	130	130	2.3	1.8
3.00	0.377	0.016	0.008	0.022	0.47	130	130	2.3	1.9
4.00	0.679	0.016	-0.012	0.022	0.47	130	130	2.3	1.9
1.17	0.057	-0.021	0.073	-0.012	-0.15	190	100	1.5	3.3
2.00	0.196	-0.014	0.225	-0.012	-0.22	210	120	1.6	3.8
4.00	0.811	-0.013	0.938	-0.012	-0.23	215	120	1.7	3.8

and by Nozières.¹⁵ The former analysis yields electrons of mass $0.05m_0$ and holes of mass $0.07m_0$, while the latter yields electrons of mass less than $0.05m_0$ and holes of mass between $0.06m_0$ and $0.07m_0$. Further evidence for the simultaneous presence of electrons and holes is the fact that the Hall coefficient changes sign as a function of magnetic field strength.²³ As the character of the de Haas-van Alphen effect is determined by the properties of the band structure near the maximum cross section of the Fermi surface, we may neglect the fine structure associated with the parameter γ_3 (at least in the orientation here considered, in which the magnetic field is parallel to the c_0 axis). We also neglect the parameter γ_4 as it causes no qualitative change in the band structure. Neglect of γ_4 may cause a 10% error in the other quantities and it should be taken into account in later, more accurate treatments. With these approximations, we are left with a four-parameter band model. In discussing a particular experiment we must add another unknown, the Fermi energy, as we cannot be sure that the sample is absolutely pure. In principle we could get six pieces of information from the experiment (the three quantities discussed above for each type of carrier), which would then determine the five unknowns and provide one test relation. In practice the longitudinal-to-transverse mass ratios turn out to be of little use in determining parameters, but do provide a consistency check. Thus, we are left with four relations among five unknowns, and we shall proceed by assuming values for γ_0 and solving for the other parameters.

The easiest way to work out the important quantities for graphite is to use the relation $\gamma_0^2\sigma^2 = (E - E_3) \times (E - E_2)$, which is actually the secular equation for the four-parameter band structure. We use the convention of letting ξ run over a double zone as discussed in Sec. 2. We shall write f_1 and f_2 for the quantities $\zeta - E_2$ and $\zeta - E_3$ evaluated at the maximum cross section of the Fermi surface for electrons. The analogous quantities for holes are written as f_3 and f_4 . It is convenient to calculate σ^2 from A by the rule σ_m^2

$= 3a_0^2 A_m / 4\pi = 3a_0^2 / (2P\hbar c)$. Shoenberg's periods of 2.20×10^{-5} and 1.65×10^{-5} gauss⁻¹ for electrons and holes, respectively, then give

$$\text{for electrons, } f_1 f_2 = 6.3 \times 10^{-4} \gamma_0^2; \quad (3.4a)$$

$$\text{for holes, } f_3 f_4 = 8.4 \times 10^{-4} \gamma_0^2. \quad (3.4b)$$

For the transverse mass we have $m_{\perp}/m_0 = (2\hbar^2/3m_0 a_0^2) \times \partial\sigma^2/\partial E = 0.839\partial\sigma^2/\partial E$. Thus, we find that

$$\text{for electrons, } f_1 + f_2 = 4.3 \times 10^{-2} \gamma_0^2; \quad (3.5a)$$

$$\text{for holes, } f_3 + f_4 = -8.3 \times 10^{-2} \gamma_0^2. \quad (3.5b)$$

In writing formulas (3.5), we have used the choice of Shoenberg's masses quoted above, and explicitly written the hole mass as negative. Even without specifying the form of E_2 and E_3 , we can immediately solve Eqs. (3.4) and (3.5) for the f 's in terms of γ_0 . It turns out that there is no solution possible for a γ_0 less than 1.17 ev.

We must distinguish two cases, depending upon the sign of γ_2 . For positive γ_2 , the maximum σ^2 for holes comes at $\xi = 2\pi$ and the maximum σ^2 for electrons is given by $\cos(\frac{1}{2}\xi_m) = \gamma_1 f_2 / 2\gamma_2 f_1$. Using these expressions for ξ , Eqs. (2.1) for E_2 and E_3 , and the values of the f 's found from above, we obtain five equations in five unknowns (counting ξ_m for electrons) for each value of γ_0 . The set of equations can be simplified and easily solved, the results being given in Table I. For negative values of γ_2 , the maximum σ^2 for electrons is at $\xi = 0$, and that for holes is given by $\cos(\frac{1}{2}\xi_m) = \gamma_1 f_4 / 2\gamma_2 f_3$. The method of solution is the same as before and the results are also given in Table I.

Several qualitative features of the results can be understood easily. In the case of positive γ_2 and for γ_0 a little larger than the minimum value, all the holes are in a region where E versus σ looks parabolic. In this case the "Fermi energy" for holes ($2\gamma_2 - \zeta$) is completely determined by m_{\perp} and σ^2 , both of which are given by experiment. Thus, $2\gamma_2 - \zeta$ is independent of γ_0 and equal to Shoenberg's value of 0.010 ev. The same sort of result holds for electrons, but as the maximum is near the crossing of E_2 and E_3 (where E is linear in σ) the convergence is slower, and the asymptotic ζ is not

²³ D. E. Soule, Bull. Am. Phys. Soc. Ser. II, I, 255 (1956).

equal to Shoenberg's value of 0.014 ev. The important quantity $2\gamma_2$ which is the total band overlap, varies little and thus is well determined by the present analysis. Near $\sigma=0$ the curvature of E versus σ is proportional to γ_0^2/γ_1 . Thus, it is principally this quantity which is determined by experiment, and its value is approximately equal to 25 throughout the range of γ_0 . The value of Δ found for negative γ_2 is much larger than expected from theoretical considerations, therefore, we choose the positive sign of γ_2 .

The mass ratios as a function of γ_0 can easily be calculated from the formula

$$2\pi|\partial^2 A/\partial k_z^2| = \frac{2}{3}(c_0/a_0)^2|\partial^2\sigma^2/\partial\xi^2| \\ = 5.0|\partial^2\sigma^2/\partial\xi^2| \rightarrow m_x/m_{11}, \quad (3.6)$$

and are included in Table I. It is seen that the ratios vary little with γ_0 and therefore, cannot be used to determine γ_0 . However, we use the calculation as a consistency check. Before making comparison it is necessary to modify Shoenberg's mass ratios. Shoenberg analyzed the susceptibility on the basis of one ellipsoid for each of the oscillating contributions (he did include spin degeneracy, of course). For a positive γ_2 we have two complete hole surfaces (one for an HH edge and another of an $H'H'$ edge) and four complete electron surfaces. As the susceptibility is proportional to $(m_{11}/m_x)^{3/2}$, we should divide Shoenberg's m_{11}/m_x ratio by 4 for holes and by 16 for electrons. The factors are interchanged for negative γ_2 . Shoenberg's mass ratios are 5500 for electrons and between 350 and 10 000 for holes. Thus, for positive γ_2 the experimental mass ratios are 350 for electrons and between 90 and 2500 for holes. It is seen that the theoretical mass ratio for holes falls in the allowed range, but for electrons the theoretical value is a factor 2.5 too low. For negative γ_2 the theoretical ratio for holes is also in the allowed range (23 to 600), but the theoretical value for electrons is a factor 7 lower than the experimental value (1400). The better agreement in the first case is further evidence for the positive sign of γ_2 .

The calculated carrier concentrations are also included in the table. The exact density of states is worked out below, but we may give a quick estimate here. The number of holes per atom is approximately $\frac{2}{3}(0.092\sigma_m^2)(\Delta\xi/2\pi)$, where $\Delta\xi$ is the height of the Fermi surface. The quantity σ_m^2 is fixed by experiment, and $\Delta\xi$ is very nearly fixed by the geometry of the zone to be equal to π . Our rough estimate then gives 2.5×10^{-5} holes per atom. Since the major dimensions of the Fermi surface do not vary much with γ_0 , neither do the carrier concentrations. For comparison, Shoenberg's carrier concentrations estimated from the ellipsoid model are 3.4×10^{-5} electrons per atom and between 1.4 and 7×10^{-5} holes per atom. Note that for positive γ_2 there are excess electrons, but for negative γ_2 there are excess holes. Hall-effect data (on a different crystal than Shoenberg's but one which exhibited nearly the

same de Haas-van Alphen periods) indicate that there are excess electrons in graphite at these temperatures.²³ This fact is stronger evidence for the choice of a positive γ_2 . The carrier densities estimated from the galvanomagnetic data are about a factor 4 lower than those calculated here, being 0.54×10^{-5} electrons per atom and 0.51×10^{-5} holes per atom.²⁴ Taking into account the uncertainties in the de Haas-van Alphen data and in the analysis of the galvanomagnetic effects, the discrepancies are not considered to be serious.†

The exact density of states for the four-parameter model is easily calculated. The total number of carriers per atom inside a given energy surface is

$$n = (0.092/2\pi) \int_{\xi(1)}^{\xi(2)} d\xi \sigma^2, \quad (3.7)$$

where $\sigma^2 = (E - E_2)(E - E_3)/\gamma_0^2$ and $\xi(1)$ and $\xi(2)$ are the vertical limits of the constant-energy surface, which can be found using Eqs. (2.1). The double-zone convention is used and spin and site degeneracy are included, so that (3.7) is evaluated along one vertical edge in the double zone. The density of states per atom per energy for each branch of the energy surface on the vertical edge is

$$N(E) = \frac{0.092}{2\pi\gamma_0^2} \\ \times |[(2E - \Delta - \gamma_2)\xi - \gamma_2 \sin\xi + 4\gamma_1 \sin\frac{1}{2}\xi]_{\xi(1)}^{\xi(2)}|. \quad (3.8)$$

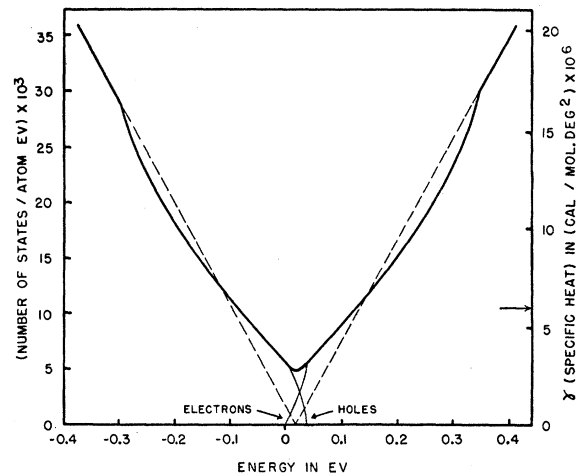


FIG. 5. The density of electronic states in graphite, calculated under the assumption that $\gamma_0 = 2$ ev. The heavy line is the total density of states, and the partial densities of states for holes and electrons are indicated. The dashed line gives the density of states for the two-dimensional model. The right-hand scale gives the predicted value of the low-temperature specific-heat constant γ , the arrow indicating the measured value.

²⁴ J. W. McClure, Bull. Am. Phys. Soc. Ser. II, 1, 255 (1956).

† Note added in proof.—An improved analysis of the galvanomagnetic data now gives carrier densities within 20% of those found in this paper.

When E is greater than $2\gamma_1 + \Delta$ or less than $-2\gamma_1 + \Delta$ the two-dimensional density of states holds:

$$N(E) = 4(0.092/\gamma_0^2) |E - \frac{1}{2}(\gamma_2 + \Delta)|. \quad (3.9)$$

Note that $\frac{1}{2}(\gamma_2 + \Delta)$ is the average energy of the four bands on the vertical zone edge. The density of states for $\gamma_0 = 2$ eV and positive γ_2 is shown in Fig. 5. The dashed line represents the two-dimensional density of states for the same γ_0 and average energy. The Wallace three-dimensional density of states with the same γ_0 and γ_1 is so nearly equal to the exact density of states that it cannot be shown clearly in the same figure. The coefficient (γ) of the linear term in the low-temperature specific heat is proportional to the density of states at the Fermi level. The scale of γ is given on the right-hand side of Fig. 5 and the arrow represents the measured value.²⁵ As the specific-heat constant is obtained by extrapolation, it is possible that the uncertainty in it is of the order of the disagreement with the theory.

4. DISCUSSION

The band parameters derived from the de Haas-van Alphen data (with a positive γ_2) are, for the most part, of the order of magnitude of the theoretical estimates discussed in Sec. 2. The one which is most out of line is γ_2 itself. However, it is the most difficult to calculate from first principles, as it depends on higher order effects. The fact that our calculated longitudinal-to-transverse electron mass ratio is a factor 2.5 too low implies that our calculated amplitude of oscillation of the susceptibility would be a factor 1.6 too low. However, the experimental mass ratio is derived by a difficult process of curve fitting, so that there is a good deal of uncertainty in the experimental value. It is gratifying that the band model constructed to fit the de Haas-van Alphen data gives rough agreement with the carrier densities estimated from galvanomagnetic data, and with the electronic specific heat. Preliminary results of Soule²⁶ on analysis of the oscillations in the galvanomagnetic properties indicate that the best values of the band parameters may be as much as 20% different from those adopted here.

The determination of all the band parameters from

²⁵ P. H. Keesom and N. Pearlman, *Phys. Rev.* **99**, 1119 (1955), Warren deSorbo (unpublished).

²⁶ D. E. Soule, *Bull. Am. Phys. Soc. Ser. II*, **2**, 140 (1957).

experiment is a problem with seven degrees of freedom (six band parameters plus the Fermi energy). Application of the de Haas-van Alphen effect reduces the number of degrees of freedom to three. This is a stroke of good luck as most other experiments would be very difficult to analyze with seven degrees of freedom. It is interesting to speculate on the remaining parameters. For instance, the fine structure caused by γ_3 is most likely the source of the abundant structure in the cyclotron resonance experiment. The minority carriers identified by Lax and Zieger could be the carriers in the projections on the Fermi surface (see Fig. 4). Nozières' interpretation of the cyclotron resonance structure differs from Lax and Zieger's, but he also uses the SW model and relies on the existence of γ_3 . Thus, we may anticipate that correct analysis of cyclotron resonance will provide a value of γ_3 . Once γ_3 is obtained, it will furnish a good idea of the value of γ_4 . The case for γ_0 may be more difficult. Firstly, for most of the carriers in pure graphite, the energy formulas contain γ_0 only in the combination γ_0^2/γ_1 . Thus, any property which depends roughly equally on all carriers will be insensitive to γ_0 . One way to obtain γ_0 is to observe effects due to states further away from the zone edge (but not so far that terms in σ^2 are important), either by doping, radiation damage, or by applying an extremely strong magnetic field. Another course is to compute the magnitude of the diamagnetic susceptibility. It has been demonstrated that a large susceptibility can result from interband transitions near a degeneracy point.¹⁶ Thus, the largest contribution to the susceptibility may come from near the crossing of E_2 and E_3 , where the energy depends on γ_0 explicitly. It should be pointed out that a preliminary investigation of the susceptibility calculation seems to imply that a value of γ_1 as large as accepted here quenches the large susceptibility calculated on the two-dimensional model. This has led Hearing and Wallace²⁷ to make an entirely different interpretation of the de Haas-van Alphen effect.

It is a pleasure to acknowledge interesting and helpful conversations on the subject of this paper with Dr. J. A. Krumhansl, Dr. J. C. Slonczewski, Dr. B. Lax, and Dr. P. P. Nozières.

²⁷ R. R. Hearing and P. R. Wallace, *J. Phys. Chem. Solids* (to be published).